

N84 15601

D11

PROPAGATING PLANE HARMONIC WAVES THROUGH FINITE LENGTH PLATES
OF VARIABLE THICKNESS USING FINITE ELEMENT TECHNIQUES

J. H. Clark, A. J. Kalinowski, C. A. Wagner

NAVAL UNDERWATER SYSTEMS CENTER
NEW LONDON, CONNECTICUT 06320

ORIGINAL PAGE IS
OF POOR QUALITY

SUMMARY

Closed form solutions exist in the literature for propagating plane harmonic waves through infinitely long uniformly thick plates which are immersed in fluids. These solutions fail to account for the edge effects present in finite length plates and address only plates of uniform thickness. This paper presents an analysis using finite element techniques which addresses the propagation of a uniform incident pressure wave through a finite diameter axisymmetric tapered plate immersed in a fluid. The approach utilized in developing a finite element solution to this problem is based upon a technique for axisymmetric fluid structure interaction problems presented in the Tenth NASTRAN Conference (ref. 1).

The problem addressed in this paper is that of a 10 inch diameter axisymmetric fixed plate totally immersed in a fluid. The plate increases in thickness from approximately 0.01 inches thick at the center to 0.421 inches thick at a radius of 5 inches. Against each face of the tapered plate a cylindrical fluid volume has been represented extending five wavelengths off the plate in the axial direction. The outer boundary of the fluid and plate regions have been represented as a rigid encasement cylinder as was nearly the case in the physical problem.

The primary objective of the analysis is to determine the form of the transmitted pressure distribution on the downstream side of the plate. A secondary purpose is to demonstrate the feasibility of employing the ref. 1 fluid-structure interaction technique on a large D.O.F. problem, and in fact running this large problem uncovered a basic error in the NASTRAN coding for 32 bit machines (e.g., VAX or IBM 360, 370, or 3033) when employing MPC or DMIG cards. These errors could impact any rigid format.

The finite element model used consists of 7455 nodes comprising 7191 axisymmetric ring elements. Both the fluid and the plate structure have been represented using axisymmetric CTRAPAX and CTRIAAX elements. The fluid (sea-water) elements and structure (plate) elements are linked together along their boundary by utilizing a duplicate set of nodes and a direct matrix insertion capability within NASTRAN. This enables the incorporation of the stiffness and mass coupling terms in the stiffness and mass matrices respectively.

The plate is loaded with a uniform harmonic pressure wave ($f = 100,000$ Hz)

which propagates axially through the incident side fluid, into the plate, and then out into the transmitted side fluid.

Presented results consist of plots of pressure along both the incident and transmitted surfaces of the tapered plate. In addition, pressure and phase contours throughout the modeled fluids are presented.

SYMBOLS

Values are given in both SI and U.S. Customary Units. The measurements and calculations were made in U.S. Customary Units.

ΔA = associated area (eq. (1))

c = value of term entered on diagonal of damping matrix

c_f = sound wave velocity in fluid

f = frequency of propagating wave

k_f = bulk modulus of the acoustic fluid

n_r = normal to a surface in radial direction

n_z = normal to a surface in axial direction

U_z = displacement in axial direction

ρ_f = mass density of acoustic fluid

INTRODUCTION

Sternberg, et al., (ref. 2) have experimentally demonstrated the frequency independent characteristics of acoustic filter plates with regards to beamforming characteristics. Mathematical approaches have been undertaken to analytically account for this phenomena with varying degrees of success. The objective of this project was to utilize the finite element method to model the transmission of a plane harmonic wave through a filter plate of variable thickness immersed in sea water. This filter plate effect, if used in conjunction with an acoustic lens, develops beams which are independent of frequency and of constant width. A typical configuration is shown in Figure 1 and has been experimentally tested.

The analysis presented accounts for the rigid containment cylinder, the tapered circular steel filter plate, the transmission side fluid inside the

containment cylinder and the incident side fluid which theoretically extends to infinity. The rubber acoustic lens discussed briefly above has been excluded from this analysis in order to isolate the effects of the filter plate.

Since the actual structure is axisymmetric the finite element model utilized is also axisymmetric. The filter plate has been analyzed by using the displacement method within NASTRAN. The fluid has been modeled in accordance with an axisymmetric pressure analogy (ref. 1). The driving force consists of a plane harmonic wave at 100 kHz at normal incidence to the steel plate. Pressure and phase distributions throughout the incident and transmitted fluid volumes are to be computed. To enhance the presentation of the rather extensive pressure and phase data, pressure and phase contours throughout the internal and external fluid have been presented. In addition, plots of pressure along the incident and transmitted surfaces of the filter plate are presented.

Model Development

As detailed in ref. 1 the development of a finite element model for any axisymmetric fluid structure interaction problem requires several steps. For large degree of freedom problems model sizing, element sizing, and element selection are reasonably straightforward, however, they must be addressed cautiously in order to avoid both technical misjudgments and excessive computer cost.

I. Sizing. The particular piece of hardware modeled is well defined. As shown in Figure 2 the encasement cylinder is 5" (12.7 cm) in length and 0.5" (1.27 cm) thick. The filter plate is 10" (25.4 cm) in diameter and tapers from .08" (0.203 cm) at the center to 0.421" (1.06 cm) at a 4" (10.16 cm) radius. The location of the driving surface is 2.5" (6.35 cm) away from the filter plate surface and at the end of the containment cylinder. The area between the filter plate and driving surface is fluid filled. On the downstream side the modeled fluid extends to the end of the containment cylinder. The fluid within the containment cylinder extends 4 wavelengths off the plate.

The important aspect relating to element sizing for steady state fluid structure interaction problems is that the distribution of nodes throughout the model be such that plane harmonic waves at the frequency of interest can adequately be described. As developed in ref. 3 adequate representation of the pressure waves is ensured by using ten nodes per wavelength or in this case where $f = 100$ kHz the node spacing becomes 0.06" (0.152 cm). This is based upon a wave propagation velocity in seawater of 60000 in/sec (152400 cm/sec). With node spacings this small and a model geometry as described above, the number of degrees of freedom approaches the limits of COSMIC NASTRAN on the VAX 11/780.

Since an axisymmetric pressure analogy solution has been invoked for the fluid elements, the selection of mating element type is limited. Several axisymmetric elements exist within COSMIC NASTRAN, however, previous success with CTRAPAX and CTRIAAX elements determined selection. These elements have been used to represent both the fluid and filter plate. As will be discussed in the

next section, the containment cylinder and driving surfaces are represented as boundary or load conditions. The finite element model developed according to the above discussion is shown in Figure 3.

II. Boundary Condition. The boundary condition addressed next is the coupling of the fluid elements (modeled within an axisymmetric pressure analogy) to the structure elements (modeled within the displacement method). This coupling when using axisymmetric elements requires duplicate nodes along any fluid structure boundary. These duplicate nodes are then utilized in formulating the off diagonal coupling terms within both the mass and stiffness matrices for each of the elements involved. The details of the coupling procedure are given in ref. 1 and are not repeated here.

The mass terms are given as, $- A^w \rho_f k_f n_r$ and $- A^w \rho_f k_f n_z$ (1)

and stiffness terms are given as, $\Delta A n_r$ and $\Delta A n_z$

The physical nature of the filter plate hardware enables representation of the cylindrical containment cylinder as a rigid outer fluid boundary condition, and is expressed as

$$\frac{\partial p}{\partial n} = 0$$

where p is the fluid pressure.

This boundary condition is implemented within the pressure analogy by freeing all constraints along the containment cylinder/fluid interface (i.e., no surface tractions).

The external fluid boundary is terminated with fluid dampers in such a way that the fluid appears to extend to mathematical infinity. Since NASTRAN does not contain any axisymmetric dashpot elements, this effect was developed using a direct matrix insertion technique similar to that required along the fluid/structure boundary. To each node along the fluid boundary the magnitude of the lumped damping term to be inserted in the damping matrix is given as

$$c = \frac{\Delta A^b k_f}{C_f}$$

As with the stiffness and mass terms described previously, the location of the damping term within the damping matrix is developed in ref. 1.

III. Loading. Plane harmonic pressure waves will be the predominant load type seen by the filter plate. The plane harmonic wave utilized in this problem is at a frequency of 100 kHz and has a magnitude of 1 psi (6895 P). This wave emanates from the outer fluid boundary parallel to the flat metal surface and impinges on the filter plate at normal incidence. The boundary conditions and loading scheme are shown in Figure 3.

ORIGINAL PAGE IS
OF POOR QUALITY

DISCUSSION

Initial attempts to execute NASTRAN and develop solutions for the pressure field resulting from the tapered filter plate were unsuccessful. Several out of the ordinary problems were encountered while making these initial checkout computer runs. The first of these relates to the use of the DMIG card or MPC card option with larger problems on a 32 bit machine (in this case the VAX 11/780).

After considerable time and expense, it was discovered that the problem arises when a model has a large number of nodes such that the combined row and column internal node number exceeds 2^{32} (the 32 bit word can no longer represent an unsigned integer of this size). As a result when NASTRAN attempts to order the list of row and column ID's in a monotonically increasing order, the large internal node numbers actually appear as smaller negative numbers because the sorting routine processes the 32nd bit as a plus or minus sign. As a result the DMIG card coupling terms were arbitrarily associated with a node elsewhere in the matrix thus voiding the coupling effect. Coding changes were suggested by RPK Corporation and ultimately corrected this error. The coding change alters the internal node sorting routine in such a way that the 32nd bit is read as part of the node number and not as a plus (+) or minus (-) sign. Subsequent runs demonstrated proper placement of the DMIG card coupling terms.

The second, less serious problem encountered relates to the mass distribution for elements which are very close to the centerline.

NASTRAN calculates the lumped mass of any axisymmetric element by first determining the centroid of the elements nodes. This radius is then used to determine the circumference of the ring element. Knowing the length and height of the element then enables a determination of the area and therefore mass of the entire ring element. This mass is allocated equally to each of the four nodes comprising the elements connectivity. For large radii this allocation scheme is very accurate, however, when the radius to the centroid of the element is less than five times the node spacing significant errors result (as much as 40%). This error has been corrected by using the elements outer and inner radii to calculate ring areas relative to the centroidal radius. This divides each ring element into an outer annulus and an inner annulus. The mass of the outer annulus is allocated to the two outer annulus nodes. The mass of the inner annulus is allocated to the two inner nodes. The FORTRAN coding changes made to the TRAPAD and TRIAAD subroutine in NASTRAN are shown in Figures 4 and 5. The lines that have changes are mainly in the lines without the column 73-80 card number designators.

RESULTS

The NASTRAN solution to a steady state fluid structure interaction problem consists of the pressure and phase distribution throughout the fluid. For very large problems this data is cumbersome to interpret, consequently two data pre-

sentations have been developed. The first consists of a plot of the pressure along the upstream and downstream sides of the tapered metal plate. This data shown in Figures 6 and 7 show several areas of higher pressure transmission through the tapered plate. The major peak to peak fluctuations along the plate surface in the pressure plots correlate with the submerged plate flexure wavelengths existing in a constant-thickness submerged plate whose thickness is the average type thickness.

A finer mesh distribution radially along the centerline is needed in order to properly model the stiffness in the plate and thus pick up the transmitted pressure. This is why the transmitted and incident pressures are too large at the centerline. Subsequent runs with a fluid plate (field solution is known) demonstrated that this error near the centerline was localized to two or three elements.

A second and, in this case, more useful presentation of this data is a color graphics format of pressure and phase contours. Pressure contours are shown in Figure 8. A noticeable effect depicted by these pressure contours is the redirection or focusing of the pressure towards the centerline. Equally important, the appearance of annular regions of increased energy transmission are evident. There are regions where more energy transmits through the plate than in similar neighboring regions. The phase contour shown in Figure 9 is evidence of the transmission of an actual plane wave from the driving boundary through the incident side fluid. The bands of constant and repeating phase angles verify this plane wave. The discontinuities in the phase contours in the downstream fluid correlate with certain redirected pressure contours evident in Figure 8. These acoustic characteristics of filter plates, while experimentally verified, have not been readily predictable. The technique utilized here establishes a reasonable prediction capability. The development of a predictive capability for both the redirection of the pressure field and the regions of higher energy transmission were objectives of this effort.

REFERENCES

1. Kalinowski, A. J., and Nebelung, C. W., "Solution of Axisymmetric Fluid Structure Interaction Problems with NASTRAN" (U), 10th NASTRAN User's Colloquium, NASA CONF Publication 2249, 1982.
2. Sternberg, R. L., and Anderson, W. A., "A Comparison of the Useful Aperture Diameter, Directivity Index and Beam Width for an Acoustic Lens and an Acoustic Lens-Acoustic Filter Plate Combination", Naval Underwater Systems Center Technical Memorandum No. 771187.
3. Kalinowski, A. J., and Nebelung, C. W., "Media-Structure Interaction Computation Employing Frequency Dependent Mesh Sizes with the Finite Element Method", Shock and Vibration Bulletin, Vol. 51, 1981.

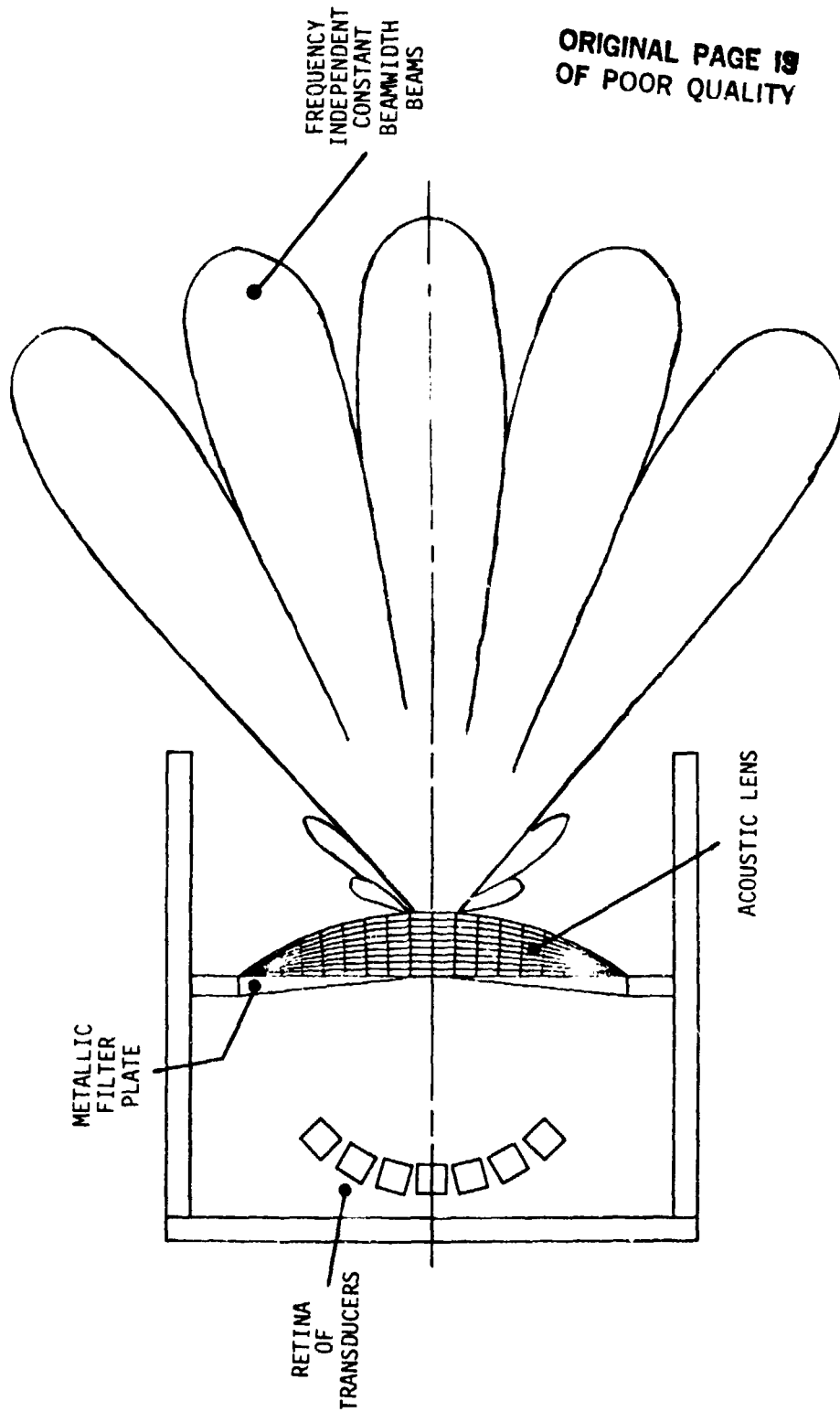


FIGURE 1 A TYPICAL TAPERED FILTER PLATE AND ACOUSTIC LENS CONFIGURATION

ORIGINAL PAGE 18
OF POOR QUALITY

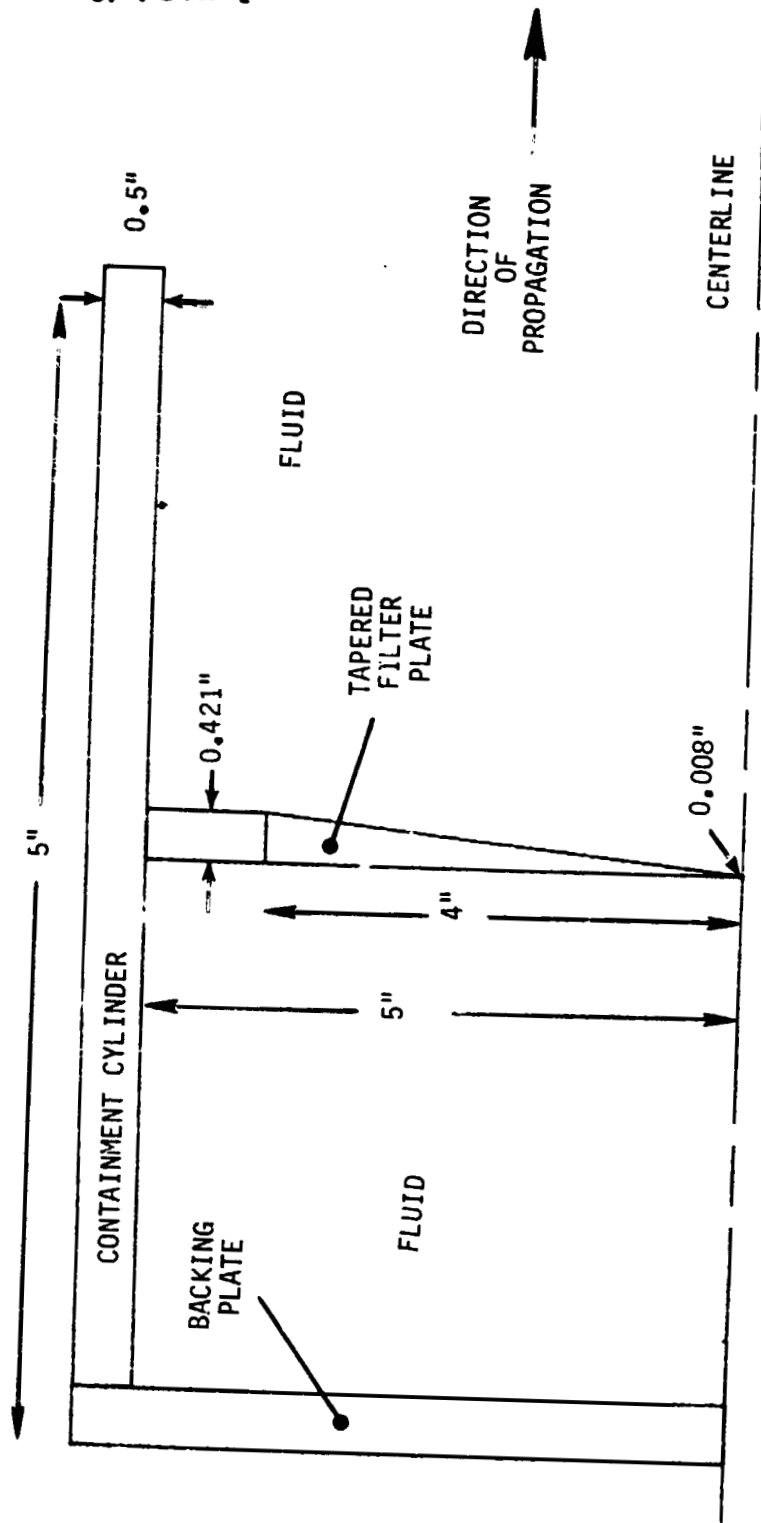


FIGURE 2. THE TAPERED FILTER PLATE AND ASSOCIATED HARDWARE

ORIGINAL PAGE 19
OF POOR QUALITY

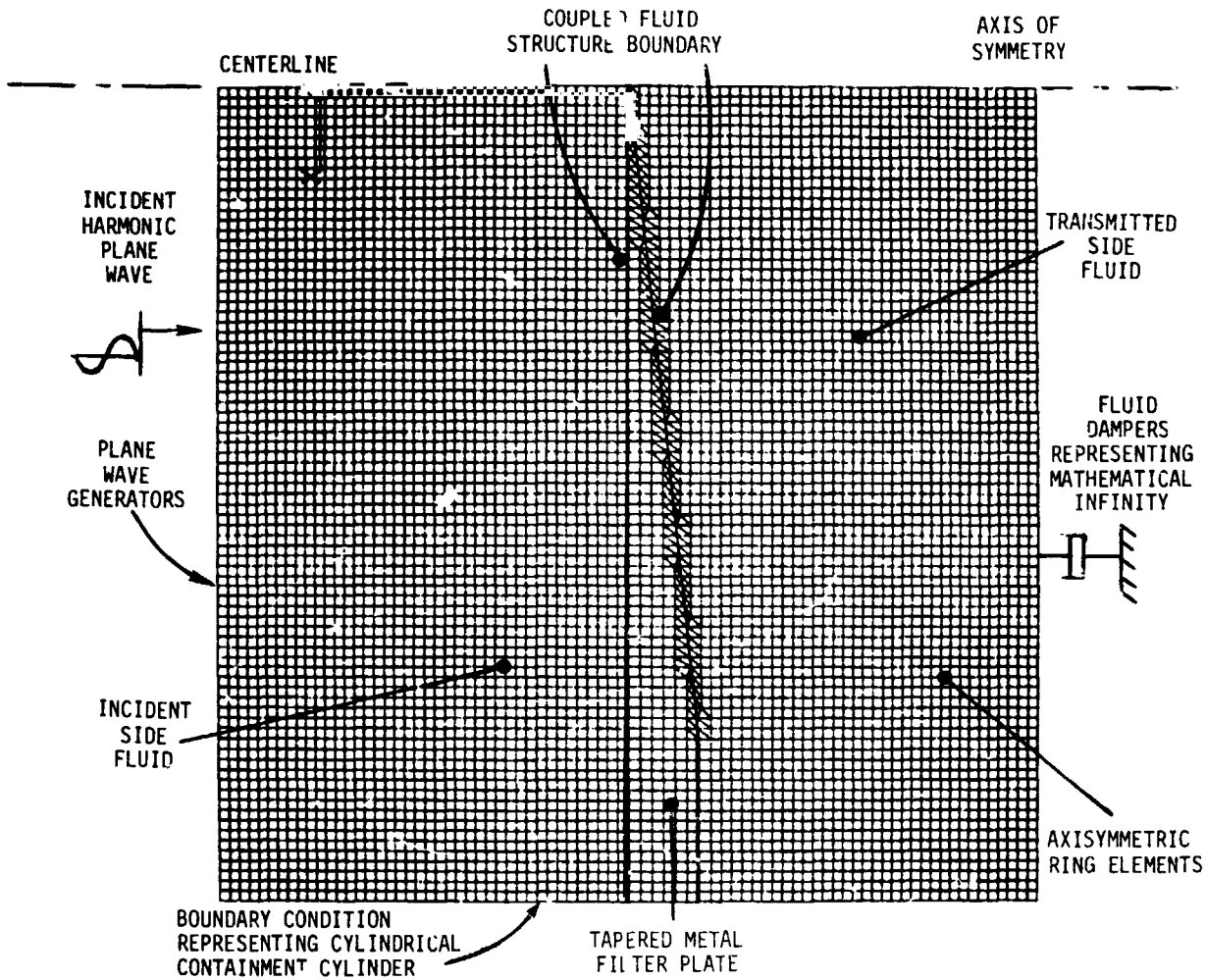


FIGURE 3. A FINITE ELEMENT MODEL OF THE TAPERED FILTER PLATE, SURROUNDING FLUID, AND STRUCTURAL BOUNDARIES

ORIGINAL PAGE IS
OF POOR QUALITY

```

C          C2,C3,C4, ... ,M,UPO,RMO          0000420
S          BR, PKI                            0000430
6,R2P,R3P,Z2P,Z3P,ARI4,FMAS1,FMAS14,FMAS23,FMAS5(4)
  NIMENSTON  (ECPT(30)),ICS(4),ECPT(20),NODNUM(4),JECPT(5)      0000440
  ...                                            0000450

EQUIVALENCE (ECPT(1), ... ,IDFL), (FMAS(1), ... ,FCPT(1)),BMBS(1)) 0000460
EQUIVALENCE (DICT5,DICT(5))                          0000460
EQUIVALENCE (IRAF1,ECPT(1))
EQUIVALENCE (JECPT(2),ECPT(2)),(JECPT(3),ECPT(3)),(JECPT(4),
  ECPT(4)),(JECPT(5),ECPT(5))
  T SORT = 0                                           0000470
  MASOT                                              000047

C
C          GENERATE LUMPED MASS MATRIX HERE          00004670
C
C          670  JFTLI=0
C          DO 690 J=1,3                               00004680
C          690  JFTLI=J                               00004690
C          690  JFTLI=J                               00004700
C*****
C          CHANGES AS PER AJK 10/12/82
C*****
C          NMTNXX=NMTNO(NODNUM(1),NODNUM(2),NODNUM(3))
C          DO 9999 JJ=1,3
C*****
C          SORT NODE NUMBERS ACCORDING TO SIZE - SMALLEST FIRST
C*****
C          IF (NMTNXX.E0.NODNUM(JJ)) GO TO 9998
C          GO TO 9999
C          9998 JFTL2=JFTLI+1
C          JFTL2=JJ
C          GO TO 9997
C          9999 CONTINUE
C          WRITE(6,9992)JFTL2,IRAFEL
C          9992 FORMAT(1X,' HAVING TROUBLE FILLING LUMPED MASS MATRIX IN TRIAD SU
  IRROUTINE, JFTL =',I2^,4X,'FL NUMBER =',I20)
C          9997 AKJM((JFTLI-1)*3+1)=FMAS(JFTL2)
C          AKJM((JFTLI-1)*3+2)=FMAS(JFTL2)
C          AKJM((JFTLI-1)*3+3)=FMAS(JFTL2)
C*****
C          STRIKE NODE OUT OF ORDERING (LOW TO HIGH) OPERATION
C*****
C          NODNUM(JFTL2)=1E+9

C*****
C          END CHANGES
C*****
C          680 CONTINUE
C          DICT(2) = 2                                00004720
C          CALL EMGOUT(AKJM,AKJM,9,1,DICT(2)          00004730
C          RETURN                                     00004740
  
```

FIGURE 4 FORTRAN CODING CHANGES IN NASTRAN SUBROUTINE TRAPAD FOR CTRAPAX ELEMENTS

ORIGINAL PAGE IS
OF POOR QUALITY

```

C      LUMPED MASS CALCULATIONS HANDLED HERE
C
900 AR = (R(1)*(Z(2)-Z(4)) + R(2)*(Z(3)-Z(1)) + R(3)*(Z(4)-Z(2)) +
X      R(4)*(Z(1)-Z(3)))/ 2.
C *** AKJ(1) = RHO*(R(1)+R(2)+R(3)+R(4))/4. * AP
C *** AKJ(1)=AKJ(1)/4.0D0
C *** DO 920 I=2,17
C 920 AKJ(I) = AKJ(1)
C
C
C FNAS14 = MASS OF HALF NEAR CENTERLINE
C FNAS23 = MASS OF HALF AWAY FROM CENTERLINE
C
R3P = (R(4) + R(3))/2.0D0
R2P = (R(1) + R(2))/2.0D0
Z3P = (Z(4) + Z(3))/2.0D0
Z2P = (Z(1) + Z(2))/2.0D0
AR14 = (R(1)*(Z2P - Z(4)) + R2P*(Z3P - Z(1))
S      + R3P*(Z(4) - Z2P) + R(4)*(Z(1) - Z3P))/2.0D0
FMAST = RHO*(R(1) + R(2) + R(3) + R(4))*AP/4.0D0
FNAS14 = FMO*(R(1) + R2P + R3P + R(4))*AR14/4.0D0
FNAS23 = FMAST - FNAS14
C****
C      CHANGES AS PER AJK 10/12/87
C****
C      COMPUTE LUMPED MASS AT NODES A,B,C,D (i.e. 1,2,3,4)
FNMAS(1)=FNAS14/2.0D0
FNMAS(2)=FNAS23/2.0D0
FNMAS(3)=FNAS23/2.0D0
FNMAS(4)=FNAS14/2.0D0
NODNUM(1)=JECPT(2)
NODNUM(2)=JECPT(3)
NODNUM(3)=JECPT(4)
NODNUM(4)=JECPT(5)
C      WRITE(6,*) ' NODNUM IN TRAPAD',NODNUM(1),NODNUM(2),NODNUM(3),
C      NODNUM(4)
JFTL=0
DO 970 I=1,4
NMTYX=MIN0(NODNUM(1),NODNUM(2),NODNUM(3),NODNUM(4))
DO 9999 JJ=1,4
C****
C      SORT NODE NUMBER ACCORDING TO SIZE (SMALLEST FIRST)
C****
IF(NMINXX.F0,NODNUM(JJ)) GO TO 9999
GO TO 9999
9999 JFTL=JFTL+1
JFTL2=JJ
GO TO 9997
9999 CONTINUE
WRITE(6,9992)JFTL2,IPADFI
9992 FORMAT(1X,' HAVING TROUBLE FILLING LUMPED MASS MATRIX IN TRAPAD SU
1X'ROUTINE',T20,4X,'FL NUMBER',I20)
9997 AKJ((JFTL-1)*3+1)=FNMAS(JFTL2)
AKJ((JFTL-1)*3+2)=FNMAS(JFTL2)
AKJ((JFTL-1)*3+3)=FNMAS(JFTL2)
C****
C      STRIKE NODE OUT OF ORDERING (LOW TO HIGH) OPERATION
C****
NODNUM(JFTL2)=1E+9
170 CONTINUE
***
END THIS SET OF CHANGES

```

00006330
00006340
00006350

FIGURE 4 FORTRAN CODING CHANGES IN NASTRAN SUBROUTINE TRAPAD FOR CTRAPAX ELEMENTS

ORIGINAL PAGE IS
OF POOR QUALITY

```

4.
5.
6.
*****
C      CHANGES AS PER AJK FOR REDISTRIBUTING MASS 10/13/87
*****
7,ZBAR1,ZBAR2,ZPAR3,RPAP1,RPAP2,RPAP3,AREA12,ARFA23,AREA13
8,RAVAG12,RAVAG23,RAVAG13,CONM12,CONM23,CONM13,ENMASS(3)
C
INTEGER DICT(11),ELID,ESTID,TSORT(3)
DOUBLE PRECISION CONSTS
LOGICAL NODC, NEST
C
EQUIVALENCE (Z(1),Z(2),Z(3)), (DICT(1),
EQUIVALENCE (AKI(1),GAPAP(1,1)), (PMASS(1,1),AKM(1))
EQUIVALENCE (CONSTS(1),PT), (CONSTS(4),DFGAP)
EQUIVALENCE (IRADEL,FCPI(1))
1, (CONSTS(2),TNOPI)
EQUIVALENCE (JECPT(1),ECPT(2)), (JECPT(2),ECPT(3)), (JECPT(3),
1ECPT(4))
C
INITIALIZE
50 T=1,3
C
PMASS(0,9) = K
C0 IN 400
C 350 ARFA = (P1*(Z2-Z3) + R2*(Z3-Z1) + R3*(Z1-Z2))/2.
C      CONVM = RHOD*(R1 + R2 + R3)/3.*ARFA
350 ZBAR1=(Z(1)+Z(2)+Z(3))/3.0
ZBAR2 = ZBAR1
ZBAR3 = ZBAR1
RPAR1 = (R(1) + R(2) + R(3))/3.0
RPAR2 = RPAR1
RPAR3 = RPAR1
ARFA12 = (R(1)*(Z(2) - ZPAR3) + R(2)*(ZBAR3 - Z(1))
+RPAP3*(Z(1) - Z(2)))/2.0
ARFA23 = (RPAR1*(Z(2) - Z(3)) + R(2)*(Z(3) - ZPAR1)
+R(3)*(ZPAR1 - Z(2)))/2.0
ARFA13 = (R(1)*(ZBAR2 - Z(3)) + RPAR2*(Z(3) - Z(1))
+R(3)*(Z(1) - ZBAR2))/2.0
RAVAG12 = (R(1) + R(2) + RPAR3)/3.
RAVAG23 = (RPAR1 + R(2) + R(3))/3.
RAVAG13 = (R(1) + RPAR2 + R(3))/3.
CONM12 = RHOD*RAVAG12*ARFA12
CONM23 = RHOD*RAVAG23*ARFA23
CONM13 = RHOD*RAVAG13*ARFA13
*****
C      CHANGES FOR MASS CALCULATION AJK 10/12/87 -
*****
C      COMPUTE LUMPED MASS AT NODES A,B,C (i.e. 1,2,3)
ENMASS(1)=(CONM12+CONM13)/2.0
ENMASS(2)=(CONM12+CONM23)/2.0
ENMASS(3)=(CONM23+CONM13)/2.0
NODNUM(1)=JECPT(1)
NODNUM(2)=JECPT(2)
NODNUM(3)=JECPT(3)
C      WRITE(6,*)ZBAR1,ZBAR2,ZPAR3,RPAP1,RPAP2,RPAP3,AREA12,ARFA23,
C      1AREA13,RAVAG12,RAVAG23,RAVAG13,CONM12,CONM23,CONM13,
C      2ENMASS(1),ENMASS(2),ENMASS(3),NODNUM(1),NODNUM(2),NODNUM(3)
*****
C      END CHANGES
*****

```

FIGURE 5 FORTRAN CODING CHANGES IN NASTRAN SUBROUTINE TRIAAD FOR CTRIAAX ELEMENTS

ORIGINAL PAGE IS
OF POOR QUALITY

```
AREA = AREA12 + AREA23 + AREA13  
CCNVW = CONN12 + CONN23 + CONN13  
IF (AREA.LT.0.0) GO TO 7171  
GO TO 7172
```

```
7171 PRINT 7173, AREA, IFCPT(1)  
7173 FORMAT(1X, 'NEGATIVE AREA = ', E11.5, 2X, 'IN ELEMENT NUMBER',  
8I15, 2X, 'DID YOU NUMBER ELEMENT COUNTER CICKWISE AS REOUTRED ??'//  
&)
```

```
C STOP  
7172 CONTINUE
```

```
00003840  
00003850  
000030
```

```
TRANSFORM THE ELEMENT STIFFNESS  
TRIC POINT DEGREE OF
```

```
SYSTEM
```

FIGURE 5 FORTRAN CODING CHANGES IN NASTRAN SUBROUTINE TRIAAD FOR CTRIAAX ELEMENTS

ORIGINAL PAGE IS
OF POOR QUALITY

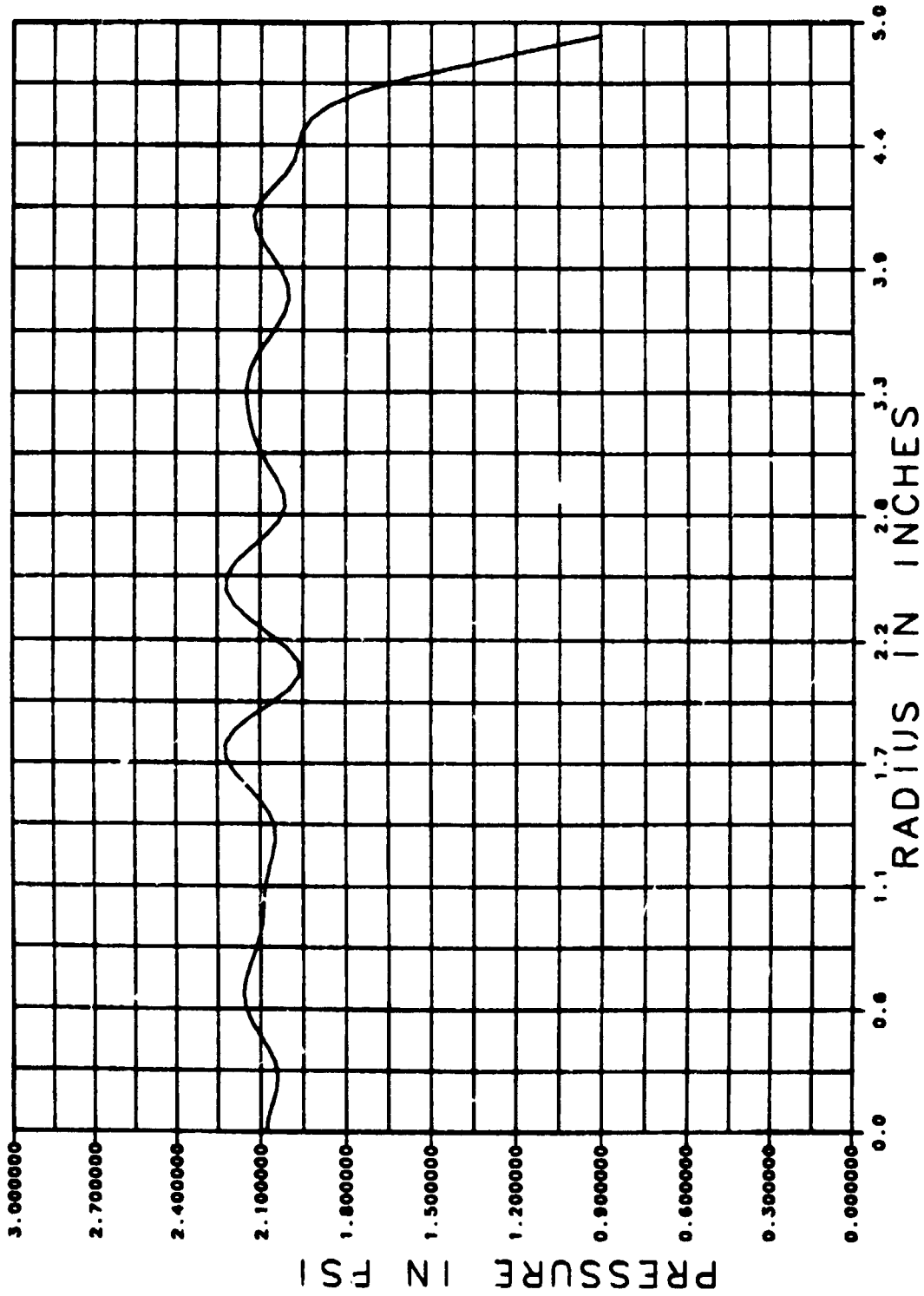


FIGURE 6 THE PRESSURE DISTRIBUTION AS A FUNCTION OF RADIUS ALONG THE INCIDENT FACE
OF THE TAPERED FILTER PLATE

ORIGINAL PAGE IS
OF POOR QUALITY

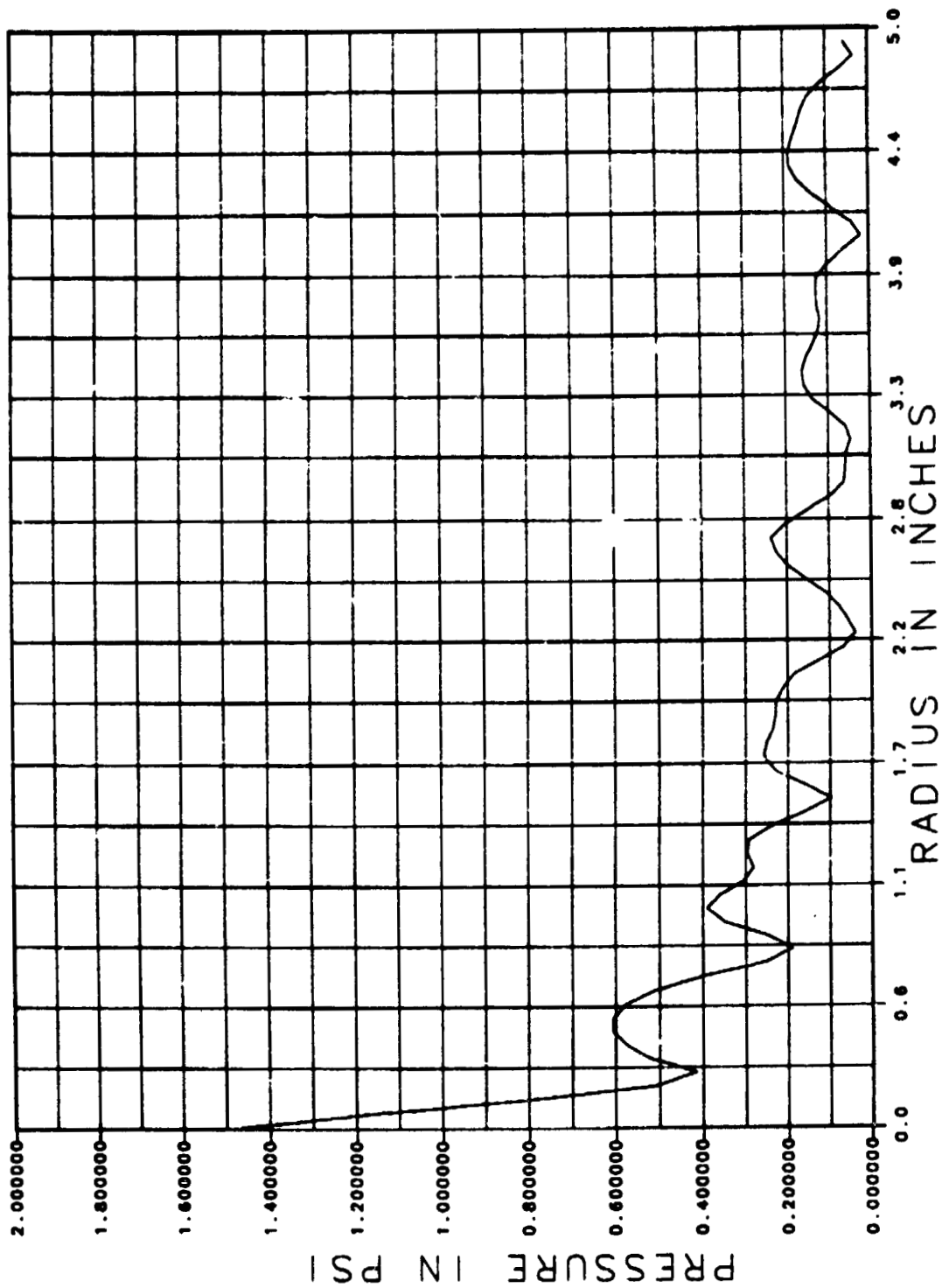


FIGURE 7 THE PRESSURE DISTRIBUTION AS A FUNCTION OF RADIUS ALONG THE TRANSMITTED
FACE OF THE TAPERED FILTER PLATE

ORIGINAL PAGE IS
OF POOR QUALITY

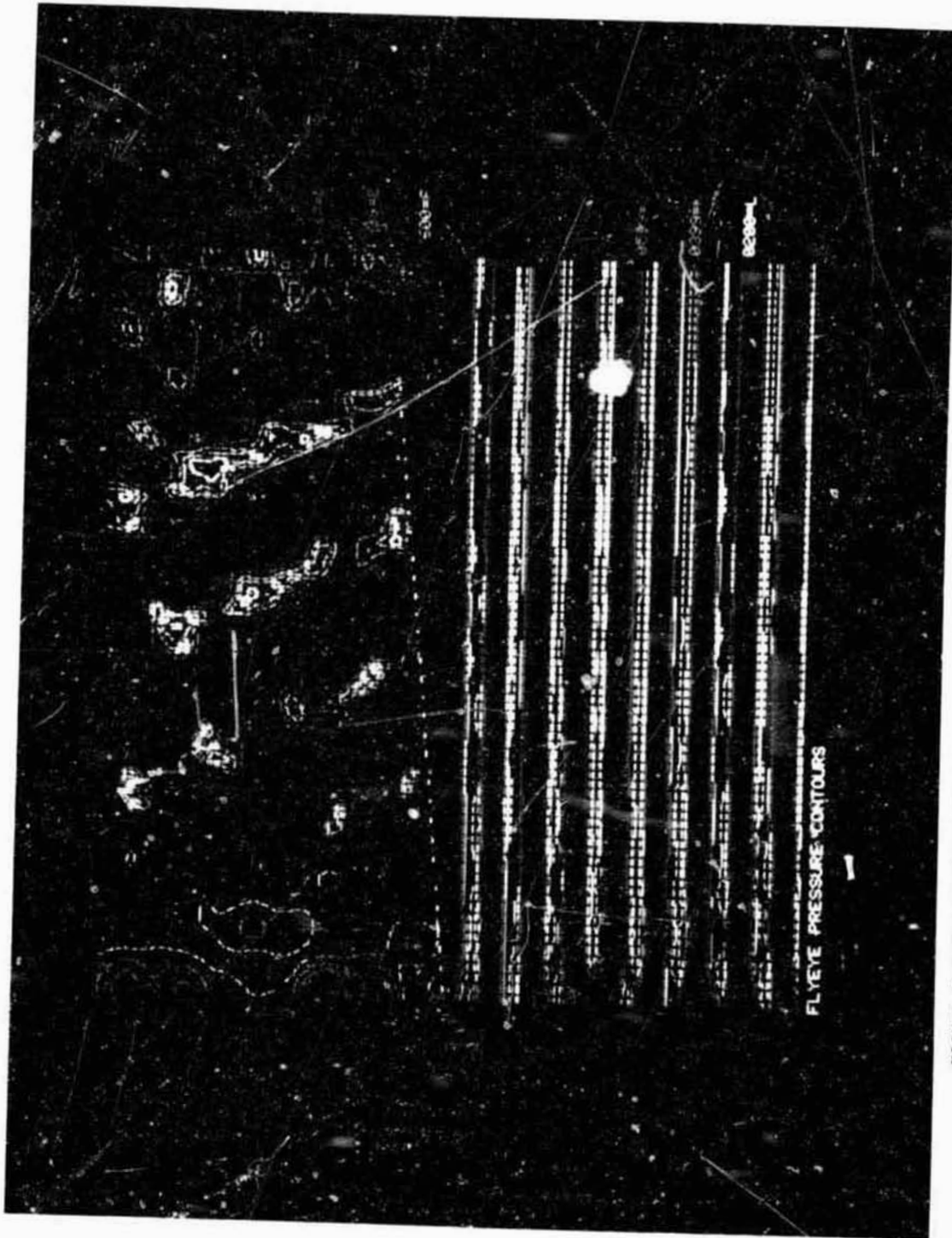


FIGURE 8 COLOR CONTOURS OF THE PRESSURE DISTRIBUTION THROUGHOUT THE TAPERED FILTER
PLATE MODEL.

FLYEYE PRESSURE CONTOURS

ORIGINAL PAGE 19
OF POOR QUALITY

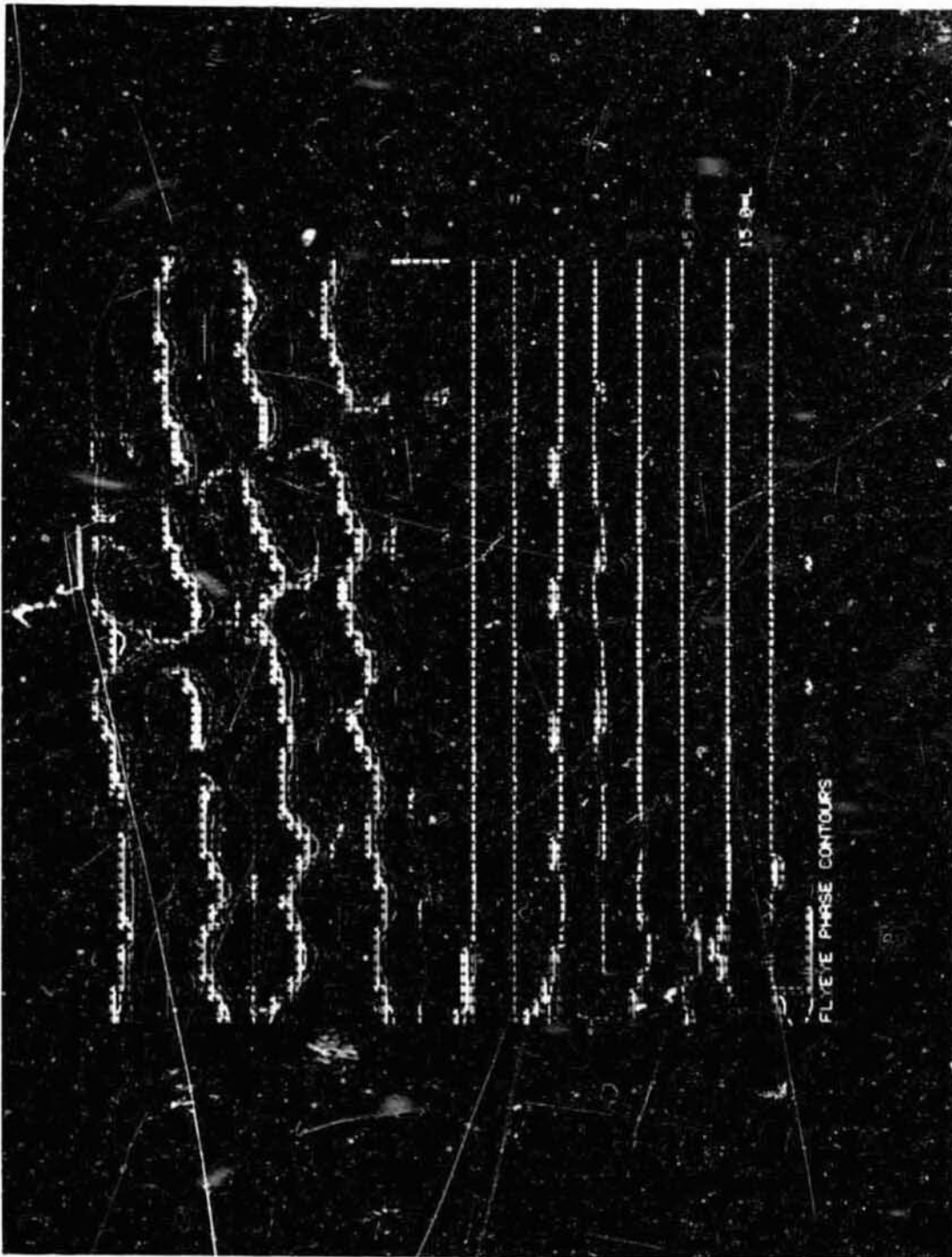


FIGURE 3 COLOR CONTOURS OF THE PHASE DISTRIBUTION THROUGHOUT THE TAPERED FILTER
PLATE MODEL